Spatial Object Recommendation with Hints: When Spatial Granularity Matters

Hui Luo[1,†], Jingbo Zhou[*,2,3], Zhifeng Bao[1], Shuangli Li[2,4],
J. Shane Culpepper[1], Haochao Ying[5], Hao Liu[2,3], Hui Xiong[*,6]
[1]RMIT University, [2]Business Intelligence Lab, Baidu Research
[3]National Engineering Laboratory of Deep Learning Technology and Application, China
[4]University of Science and Technology of China, [5]Zhejiang University, [6]Rutgers University
{hui.luo,zhifeng.bao,shane.culpepper}@rmit.edu.au
{zhoujingbo,liuhao30,v_lishuangli}@baidu.com,haochaoying@zju.edu.cn,hxiong@rutgers.edu

ABSTRACT

Existing spatial object recommendation algorithms generally treat objects identically when ranking them. However, spatial objects often cover different levels of spatial granularity and thereby are heterogeneous. For example, one user may prefer to be recommended a region (say *Manhattan*), while another user might prefer a venue (say a *restaurant*). Even for the same user, preferences can change at different stages of data exploration. In this paper, we study how to support top-k spatial object recommendations at varying levels of spatial granularity, enabling spatial objects at varying granularity, such as a city, suburb, or building, as a Point of Interest (POI). To solve this problem, we propose the use of a *POI tree*, which captures spatial containment relationships between POIs. We design a novel multi-task learning model called MPR (short for *Multi-level POI Recommendation*), where each task aims to return the top-k POIs at a certain spatial granularity level. Each task consists of two subtasks: (i) attribute-based representation learning; (ii) interaction-based representation learning. The first subtask learns the feature representations for both users and POIs, capturing attributes directly from their profiles. The second subtask incorporates user-POI interactions into the model. Additionally, MPR can provide insights into why certain recommendations are being made to a user based on three types of hints: *user-aspect*, *POI-aspect*, and *interaction-aspect*. We empirically validate our approach using two real-life datasets, and show promising performance improvements over several state-of-the-art methods.

KEYWORDS

Spatial Object Recommendation; POI Tree; Attention Network

---

†This work was done when Hui Luo visited Baidu Research.
*Jingbo Zhou and Hui Xiong are corresponding authors.

---

1 INTRODUCTION

Spatial object recommendation is an important location-based service with many practical applications, where the most relevant venues [31, 34] or regions [21] are recommended based on spatial, temporal, and textual information. Existing spatial object recommendation methods [20, 24, 29] usually do not differentiate the granularity of spatial objects (i.e., building versus suburb), when ranking a list of top-k objects. However, the most appropriate granularity of spatial object ranking may vary at different stages of data exploration for a user, and can vary from one user to another, which is hard to predict a priori. Choosing the most appropriate spatial granularity based on the recommendation scenario is often critical [1]. For example, if a user is planning to visit America for a holiday, they may initially want to be recommended a particular region such as "Los Angeles" or "New York" at the beginning of data exploration. The user might also wish to drill down for specific venue recommendations such as a restaurant or a bar as the exploration continues.

Therefore, user expectations at varying spatial granularity of POIs (Point of Interests, i.e., a region or a venue) should be satisfied by the recommender system adaptively and dynamically. Note that a recommended region or venue is referred to as a POI for ease of readability in this paper. We refer to this as the *multi-level POI recommendation* problem, which aims to recommend the top-k POI candidates from each level of spatial granularity. Dynamic selection of the most appropriate recommendation level(s) is driven by user interactions and application constraints. Elucidating all integration-specific details of our proposed model for an end-to-end production system is beyond the scope of this paper.

To solve this *multi-level POI recommendation* problem, a straightforward solution is to build a separate recommendation model for each level of spatial granularity, and then apply an existing POI recommendation algorithm directly. However, this approach has one drawback: it may not fully leverage mutual information among POIs at different spatial granularity levels. For example, a user may prefer to visit an area because of the POIs contained in that area. Therefore, a major challenge must be addressed: *How can we achieve a one-size-fits-all model to make effective recommendations at every level of spatial granularity?* In other words, instead of designing

Figure 1: User check-in records at varying spatial granularity.

a best-match recommendation model for level independently, the spatial containment relationships between all of the levels should be considered. If a user has visited a POI p (like a shop), there will be a check-in record for the parent POI(s) (like a shopping mall) covering p. Such information can heavily influence and assist the recommendation of the parent POI(s).

In this paper, POIs are structured as a tree based on their spatial containment − defined as the relationship of a child POI which is fully covered by a higher level POI [11]. For example, a restaurant is within a mall, which in turn is within a suburb (CBD) of a city in Figure 1, allowing recommendation to be made at any level (i.e., a particular spatial granularity) in the POI tree. We then propose a new technique called MPR (short for **M**ulti-level **P**OI **R**ecommendation), which employs multi-task learning in order to jointly train the model using every available level of spatial granularity. Each task corresponds to recommending POIs located at a certain spatial granularity. Our approach is able to leverage data that is much sparser than prior work [12, 15, 24, 29], which used only the check-in metadata found in commonly datasets such as Foursquare or Gowalla. Our two test collections were generated using real-life data from an online map service which is also more heterogeneous than the collections commonly used in similar studies. Moreover, the sparsity of a user-POI check-in matrix for Foursquare and Gowalla – the most commonly used ones by existing work – is around 99.9% [18], while our datasets are much more sparse (i.e., around 99.97%), sparse, which is an essential hurdle to overcome when using real map data. In order to alleviate the sparsity issue, POI features can be propagated from bottom to top in a POI tree using an attention network mechanism, such that the information of child POI(s) can be used by a parent POI in recommendations. In essence, child POIs are learned features that contribute directly to any related higher-level POIs, and multiple levels of such a parent-child relationship can exist. In addition, it is non-trivial to consider the geospatial influence of a location when ranking a recommendation [18]. That is, users are more likely to prefer nearby locations over distant ones when they have a choice. Thus we create a *POI context graph* to describe the geospatial influence factors between any two POIs at the same level, which maps three different sources of spatial relationships — *co-search*, *co-visit*, and *geospatial distance*.

Lastly, it is worth noting that our proposed model can be used to directly justify recommendations to a user for any level of spatial granularity. Providing justification for recommendations has been shown to be an important factor in user satisfaction [2, 3]. For instance, when Alice is in a dilemma about a recommended POI, we can provide recommendation hints along with the recommended POIs, in three aspects where the latter two are unique in

Table 1: A summary of key notations. The midlines partition the variables by section − Section 2, 3, and 4 respectively.

Symbol	Description	Dimension
$\mathcal{U}, \mathcal{P}$	The set of users and POIs, respectively	
$\mathcal{I}$	The set of user-POI interactions	
$\mathcal{T}$	The POI tree with L levels	
l	The l-th level of $\mathcal{T}$	
m (or n_l)	The number of users (or POIs at the l-th level of $\mathcal{T}$	
p_i^l	The i-th POI node located at the l-th level of $\mathcal{T}$	
$C(p_i^l)$	The child POIs rooted at p_i^l	
f_u (or f_p)	The number of users' (or POIs') explicit features; $f = f_u + f_p$.	
r	The latent factor size of explicit features.	
$\mathbf{X}$ (or $\mathbf{Y}^l$)	The observed matrix between users (or POIs at the l-th level of $\mathcal{T}$) and their attributes	$\mathbb{R}^{m \times f}$ (or $\mathbb{R}^{n_l \times f}$)
$\mathbf{U}_u$ (or $\mathbf{U}_p^l$)	The explicit feature representations of users (or POIs at the l-th level of $\mathcal{T}$)	$\mathbb{R}^{m \times r}$ (or $\mathbb{R}^{n_l \times r}$)
$\mathbf{V}^T$	The shared latent explicit feature representations of both users and POIs at the l-th level of $\mathcal{T}$	$\mathbb{R}^{r \times f}$
$\mathbf{XA}$ (or $\mathbf{YA}^l$)	The direct attribute matrix of users (or POIs at the l-th level of $\mathcal{T}$)	$\mathbb{R}^{m \times f_u}$ (or $\mathbb{R}^{n_l \times f_p}$)
$\mathbf{XT}$ (or $\mathbf{YT}^l$)	The inverse attribute matrix of users (or POIs at the l-th level of $\mathcal{T}$)	$\mathbb{R}^{m \times f_p}$ (or $\mathbb{R}^{n_l \times f_u}$)
p_j^+, p_j^-	The positive and negative POI instances	
r_l	The latent factor size of implicit features at the l-th level of $\mathcal{T}$	
d_1	The hidden layer size of the attention network	
$\mathbf{O}^l$	The user-POI check-in matrix	$\mathbb{R}^{m \times n_l}$
$\mathbf{S}^l$	The feature-based check-in matrix	$\mathbb{R}^{m \times n_l}$
$\mathbf{G}^l$	The historical check-in matrix	$\mathbb{R}^{m \times n_l}$
$\mathbf{H}_u^l$ (or $\mathbf{H}_p^l$)	The implicit feature representations of users (or POIs at the l-th level of $\mathcal{T}$)	$\mathbb{R}^{m \times r_l}$ (or $\mathbb{R}^{n_l \times r_l}$)
$\mathbf{A}_p^l$	The inner-level propagated POI feature representation	$\mathbb{R}^{n_l \times r_{l+1}}$

our model. We can provide: (1) *user-aspect* hint based on the user profile: Chinatown appears to be an important area since she loves dumplings based on her user profile. (2) *POI-aspect* hint based on the POI tree: the particular region (such as the CBD) is initially recommended since it contains several relevant shops and restaurants of interest to the user. (3) *interaction-aspect* hint based on the POI context graph: the *State Library* is also recommended because she has visited a library several times before.

In summary, we make the following contributions:

- We are the first to explore the multi-level POI recommendation problem, which aims to simultaneously recommend POIs at different levels of spatial granularity (Section 2).
- We propose a novel model MPR using multi-task learning, where each task caters for one level of the spatial granularity. Each task has two subtasks: *attribute-based representation learning* (Section 3) and *interaction-based representation learning* (Section 4).
- Our model can provide specific hints on why certain POI recommendations are being made, namely *user-aspect*, *POI-aspect*, and *interaction-aspect* hints (Section 5).
- We perform extensive experiments on two large-scale real-life datasets to evaluate the performance of our model. Our experimental results show promising improvements over several state-of-the-art POI recommendation algorithms (Section 6).

2 PROBLEM FORMULATION AND MODEL OVERVIEW

Throughout this paper, all vectors are represented by bold lowercase letters and are column vectors (e.g., $\mathbf{x}$), where the i-th element is shown as a scalar (e.g., $\mathbf{x}_i$). All matrices are denoted by bold upper

case letters (e.g., $\mathbf{M}$); the element located in the i-th row and j-th column of matrix $\mathbf{M}$ is marked as $\mathbf{M}_{i,j}$. Also, we use calligraphic capital letters (e.g., $\mathcal{U}$) to denote sets and use normal lowercase letters (e.g., u) to denote scalars. Note that, the superscript l is used in certain symbols to denote the l-th level of $\mathcal{T}$, such as $\mathbf{Y}^l$. For clarity of exposition, Table 1 summarizes the key notations used in this work, where only the dimensions of matrices are reserved.

2.1 Problem Definition

In a recommender system, there are a set of users $\mathcal{U} = \{u_1, u_2, ..., u_m\}$ and a set of POIs $\mathcal{P} = \{p_1, p_2, ..., p_n\}$ available. Each user $u_i \in \mathcal{U}$ has an attribute set derived from a user profile, such as age and hobby. Each POI $p_j \in \mathcal{P}$ has two components: (i) a parent POI, indicating that p_j is covered geospatially, and the parent POI may be empty if p_j is a root area; (ii) an attribute set, which is derived from the POI profile and typically contains attributes such as a tag or category. Based on spatial containment relationships among POIs, we construct a POI tree (see Definition 1) over $\mathcal{P}$ to predict POIs for each level of spatial granularity.

Definition 1. (POI Tree) A POI tree $\mathcal{T}$ is a tree structure of L levels, where each node represents a spatial object, H_l denotes the l-th level of $\mathcal{T}$, and n_l is the number of POI nodes at level H_l. A node p_i^l is the parent of a node p_j^{l+1} if p_i^l contains p_j^{l+1} in geo-space. We denote $C(p_i^l)$ as all child POIs rooted at p_i^l. An illustrative example of a POI tree is shown in Figure 1.

User-POI Interaction. Each instance of the interaction $\mathcal{I}$ between a user u_i and a POI p_j is a tuple $\langle u_i, p_j, s_{ij} \rangle$, where the score s_{ij} corresponds to a "binary value", indicating whether u_i has visited p_j (e.g., $s_{ij} = 1$ when u_i has checked in p_j; otherwise, $s_{ij} = 0$).

Definition 2. (Multi-level POI Recommendation) Given a user, their historical user-POI interactions, a pre-built POI tree $\mathcal{T}$, and a parameter k, return the top-k most relevant POIs at each level of $\mathcal{T}$.

2.2 An Overview of the MPR Model

Model Architecture. The architecture of the model MPR is shown in Figure 2. Taking the input of historical user-POI interactions and a pre-built POI tree $\mathcal{T}$ based on spatial containment relationship, MPR outputs the top-k POIs for each level of $\mathcal{T}$. To achieve the goal shown in Definition 2, we leverage multi-task learning to implement a joint optimization over all levels of the POI tree, where each task includes two main subtasks for the given POI level: *attribute-based representation learning* (Section 3) and *interaction-based representation learning* (Section 4).

The first subtask explores the attributes of both users and POIs by mapping them to two embedding spaces: $\mathbf{X}$ and $\mathbf{Y}^l$. These are induced from two sources of information: (i) $\mathbf{XA}$ and $\mathbf{YA}^l$, which are attributes directly derived from the user and POI profile, respectively. (ii) $\mathbf{XT}$ and $\mathbf{YT}^l$, which are derived from the user and POI attribute distributions obtained from check-in statistics.

The second subtask focuses on how to model the interactions between users and POIs to further capture personal preferences. Additionally, we model two important matrices: (i) the inter-level POI features matrix $\mathbf{A}_p^l$ propogated from child POIs using an attention mechanism; and (ii) the geospatial influence matrix $\mathbf{U}_g^l$ between

POIs derived from a *POI context graph* (Section 4.2.2), each edge of which contains one of the three types of spatial relationships between any two POIs at the same level, i.e., *co-search*, *co-visit*, and *geospatial distance*.

These two subtasks are combined using shared latent factors (i.e., $\mathbf{U}_u$ and $\mathbf{U}_p^l$), in order to guarantee that the feature representations of users and POIs at the l-th level of $\mathcal{T}$ will remain unchanged despite attributes and interactions being modeled in separate subtasks.

Objective. As each task in MPR incorporates two different learning objectives for each subtask, we train a joint model by optimizing the sum of two loss functions as follows.

$$\mathcal{L} = \lambda_1 \mathcal{L}_1 + \lambda_2 \mathcal{L}_2 + ||\Theta||_F^2 \tag{1}$$

where $\mathcal{L}_1$ and $\mathcal{L}_2$ are the loss functions for the first and second objectives applied across all levels of $\mathcal{T}$. The computational details of these two loss functions are described further in Section 3 and Section 4, respectively. λ_1 and λ_2 are hyper-parameters to balance the trade-off between the two loss functions, and $||\Theta||_F^2$ is the L2 regularization used by the model to minimize overfitting, and $||\cdot||_F$ is the Frobenius norm.

3 ATTRIBUTE-BASED REPRESENTATION LEARNING

Traditional methods usually leverage historical user-POI interactions by mapping users and POIs to a shared latent space via factorization over a user-POI affinity matrix. However, the learned latent space rarely provides any insight into why a user prefers a POI [37]. Worse still, such data is often quite sparse [8], which may not be sufficient to provide meaningful signals.

To address this limitation, we leverage the attributes of both users and POIs, which provide complimentary evidences (i.e., the "user-aspect hint" introduced in Section 5) to reveal to a user why certain POIs are being recommended. This allows a user to interactively provide additional information to align the current recommendations with their information need. We refer to these attributes that can be directly derived from the dataset as *explicit features*, e.g., user's age and hobby. In contrast, *implicit features* correspond to the attributes inferred from available data. To this end, we learn an attribute-based representation for our recommender system.

3.1 Objective Loss Function

Before introducing details on model training using the above attributes, we define the first loss function to be used in our approach. Similar to previous matrix factorization models for user-POI check-in records, we derive a factorization model over the observed user-attribute matrix $\mathbf{X} \in \mathbb{R}^{m \times f}$ and POI-attribute matrix $\mathbf{Y}^l \in \mathbb{R}^{n_l \times f}$ to learn *explicit feature* representations for users and POIs, where f is the total number of explicit features of users and POIs. This can be achieved by minimizing the following loss function:

$$\mathcal{L}_1 = ||\mathbf{U}_u \mathbf{V}^T - \mathbf{X}||_F^2 + \sum_{l=1}^{L} ||\mathbf{U}_p^l \mathbf{V}^T - \mathbf{Y}^l||_F^2 \tag{2}$$

where $\mathbf{U}_u \in \mathbb{R}^{m \times r}$ and $\mathbf{U}_p^l \in \mathbb{R}^{n_l \times r}$ are two learned parameters to model the explicit feature representations of users and POIs, which are then combined with a shared latent vector $\mathbf{V}^T \in \mathbb{R}^{r \times f}$. Here, r is the latent factor magnitude.
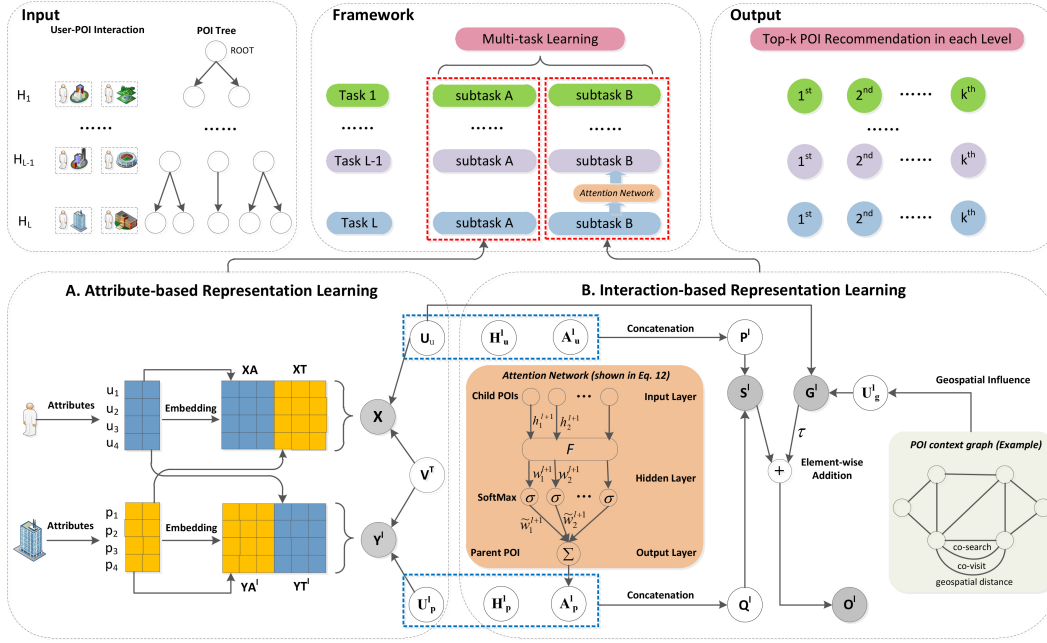
Figure 2: Architecture of the multi-level POI recommendation (MPR) model. (Best viewed in color)

3.2 Representation of User and POI Features

We first show how to build the matrix $\mathbf{X}$ to incorporate the attribute values of users. $\mathbf{X}$ is in turn a concatenation of two matrices capturing different contexts – (1) a *direct attribute matrix* $\mathbf{XA}$ directly obtained from user attributes; (2) an *inverse attribute matrix* $\mathbf{XT}$ induced from the empirical user check-in distribution:

$$\mathbf{X} = \mathbf{XA} \oplus \mathbf{XT} \qquad (3)$$

where $\mathbf{XA} \in \mathbb{R}^{m \times f_u}$, $\mathbf{XT} \in \mathbb{R}^{m \times f_p}$, $\mathbf{X} \in \mathbb{R}^{m \times f}$, $f = f_u + f_p$, and $\oplus$ is the concatenation operator.

Similarly, we construct the attribute matrix $\mathbf{Y}^l$ for POIs at the l-th level of $\mathcal{T}$, which in turn is a concatenation of a *direct attribute matrix* $\mathbf{YA}^l$ and an *inverse attribute matrix* $\mathbf{YT}^l$:

$$\mathbf{Y}^l = \mathbf{YA}^l \oplus \mathbf{YT}^l \qquad (4)$$

where $\mathbf{YA}^l \in \mathbb{R}^{n_l \times f_p}$, $\mathbf{YT}^l \in \mathbb{R}^{n_l \times f_u}$, $\mathbf{Y}^l \in \mathbb{R}^{n_l \times f}$. We use f_u and f_p to denote the number of user features and POI features generated from their respective attributes. The concatenation process is illustrated in the lower left corner of Figure 2.

Constructing the direct attribute matrix. Raw attribute values can be numerical (e.g., the age is 18) or binary (e.g., a hobby such as *reading*). We empirically define various decision rules to split an attribute a_k into two decision features. For any numerical attribute (e.g., age), a threshold θ_k is selected to split the attribute into $[a_k < \theta_k]$ and $[a_k \geq \theta_k]$. Note that, multiple threshold values can also be used to split one attribute empirically, which generates a corresponding number of features. For a binary attribute (e.g., country), we have $[a_k = \theta_k]$ or $[a_k \neq \theta_k]$.

$$\mathbf{XA}_{i,k} = \begin{cases} 1 & \text{If } u_i \text{ satisfies the decision rule over } a_k \\ 0 & \text{Otherwise} \end{cases} \qquad (5)$$

Given the attribute set of users and the attribute set of POIs located at the l-th level of $\mathcal{T}$, we model the *direct attribute matrices*

$\mathbf{XA}$ (Eq. 5) and $\mathbf{YA}^l$ (Eq. 6) as a concatenation of one-hot vectors, where an element of value 1 denotes a fulfilled decision rule.

$$\mathbf{YA}^l_{j,k} = \begin{cases} 1 & \text{If } p_j \text{ satisfies the decision rule over } a_k \\ 0 & \text{Otherwise} \end{cases} \qquad (6)$$

Constructing the inverse attribute matrix. We assume that users visit only the venues they are interested in, e.g., if Alice often goes to the library, she may be a book-lover. However, such info has to be inferred as it may not be available in the user profile (hobbies). This assumption allows us to enrich the raw data, and is a form of *weak supervision* [5]. Leveraging the attributes of POIs visited by users in this manner somewhat mitigates sparsity and cold-start issues commonly encountered in recommendation modeling.

If a POI p_j, which has an attribute a_k and was visited by a user u_i for tp_{ijk} times, then $tp_{ik} = \sum tp_{ijk}$ and each element in the user *inverse attribute matrix* $\mathbf{XT}$ is computed as follows (assume min-max normalization):

$$\mathbf{XT}_{i,k} = \begin{cases} \dfrac{tp_{ik} - tp_{ik}^{\downarrow}}{tp_{ik}^{\uparrow} - tp_{ik}^{\downarrow}} & \text{If } u_i \text{ visited } p_j \text{ that has } a_k \\ 0 & \text{Otherwise} \end{cases} \qquad (7)$$

where $tp_{ik}^{\uparrow}$ and $tp_{ik}^{\downarrow}$ are the highest and lowest check-in frequency for u_i, respectively.

Similarly, attributes for the users who checked in a specific POI p_j represent the *inverse attributes*. Suppose a POI was visited by tu_{ijk} users who have an attribute a_k, then $tu_{jk} = \sum tu_{ijk}$ and each element in the POI *inverse attribute matrix* $\mathbf{YT}^l$ is:

$$\mathbf{YT}^l_{j,k} = \begin{cases} \dfrac{tu_{jk} - tu_{jk}^{\downarrow}}{tu_{jk}^{\uparrow} - tu_{jk}^{\downarrow}} & \text{If } p_j \text{ was visited by } u_i \text{ who has } a_k \\ 0 & \text{Otherwise} \end{cases} \qquad (8)$$

where $tu_{jk}^{\uparrow}$ and $tu_{jk}^{\downarrow}$ are the largest and the smallest number of users who visit p_j, respectively.

4 INTERACTION-BASED REPRESENTATION LEARNING

In this section, we will show how to further boost the recommendation performance by exploiting user-POI interactions.

4.1 Objective Loss Function

We leverage the Bayesian Personalized Ranking (BPR) [22] principle to construct the loss function $\mathcal{L}_2$ for the second subtask. Specifically, following the popular negative sampling strategy [13, 26], a negative POI instance p_j^- which the user never visited is paired with a positive POI instance p_j^+, and the pairwise log loss can be computed by maximizing the difference between the prediction scores of the positive and negative samples. $\mathcal{L}_2$ is shown as follows:

$$\mathcal{L}_2 = -\sum_{l=1}^{L}\sum_{i=1}^{m}\sum_{j=1}^{n_l} \ln \sigma(O_{i,p_j^+}^l - O_{i,p_j^-}^l) \qquad (9)$$

where $O_{i,p_j^+}^l$ (or $O_{i,p_j^-}^l$) is the predicted score w.r.t. a positive POI p_j^+ (or a negative POI p_j^-) located at the l-th POI level for the i-th user. Here, we add the *minus* sign in the front to match the minimization objective with Eq. 1. The *user-POI check-in matrix* $O^l \in \mathbb{R}^{m \times n_l}$ will be further elaborated next.

4.2 Modeling user-POI interaction

We incorporate two matrices $S^l \in \mathbb{R}^{m \times n_l}$ and $G^l \in \mathbb{R}^{m \times n_l}$ into O^l through a linear combination, where S^l denotes the *feature-based check-in matrix*, and G^l is the *historical check-in matrix*. A configurable parameter τ is used to control the relative contributions of these two matrices, resulting in the following equation:

$$O^l = S^l + \tau G^l \qquad (10)$$

By combining S^l and G^l, we obtain the final top-k recommended results sorted by similarity score O^l. This process is illustrated in the lower right corner of Figure 2. Next, we show how to construct S^l and G^l.

4.2.1 Constructing the feature-based check-in matrix. In order to fully leverage the interaction data of users and POIs, the feature-based check-in matrix S^l located at the l-th level is built based on the feature representation P^l and Q^l w.r.t. users and POIs, respectively:

$$S^l = P^l(Q^l)^T, P^l = U_u \oplus H_u^l \oplus A_u^l, Q^l = U_p^l \oplus H_p^l \oplus A_p^l \qquad (11)$$

In Eq. 11, $P^l \in \mathbb{R}^{m \times (r+r_l+r_{l+1})}$ is a concatenation of three matrices w.r.t. users: U_u, H_u^l, and A_u^l. Specifically, U_u is the explicit feature representation of users. $H_u^l \in \mathbb{R}^{m \times r_l}$ is the implicit feature representation of users, and $A_u^l \in \mathbb{R}^{m \times r_{l+1}}$ is a trainable matrix parameter to match A_p^l in the same space. Here, r_l denotes the latent factor size of implicit features at the l-th level of $\mathcal{T}$.

Accordingly, $Q^l \in \mathbb{R}^{n_l \times (r+r_l+r_{l+1})}$ incorporates three kinds of information w.r.t. the POIs at the l-th level of $\mathcal{T}$: U_p^l is the explicit feature representation, $H_p^l \in \mathbb{R}^{n_l \times r_l}$ is the implicit feature representation, and $A_p^l \in \mathbb{R}^{n_l \times r_{l+1}}$ is the inter-level POI feature representation propagated from child POIs with an attention network.

Recall that U_u and U_p^l were described in Section 3. We now describe the details on how to construct implicit feature representations H_u^l and H_p^l, and how to produce an inter-level POI feature representation A_p^l.

Implicit feature representation. Some features that influence user preferences may be implicit. For example, Alice might go to historical libraries because she loves the classical architecture there, or for other unknown reasons which cannot be inferred. These types of features can be learned by using two matrices H_u^l and H_p^l w.r.t. users and POIs, respectively.

Inter-level propagated POI feature representation. The feature information covered by a child POI can also be used by its parent POI. For instance, the attributes of child POIs (e.g., a restaurant or a store) can be aggregated into its parent POI (e.g., a mall).

In particular, for each parent POI p_i^l, we also propagate a learned implicit feature representation (i.e., an embedding vector h_j^{l+1} in H_p^{l+1}) from each child POI p_j^{l+1} to p_i^l, producing the inter-level feature representation a_i^l for p_i^l to leverage the inter-level information. Here, we denote $A_p^l \in \mathbb{R}^{n_l \times r_{l+1}}$ as the inter-level POI feature representation matrix for all POIs at the l-th level of $\mathcal{T}$, where a_i^l is an embedding vector for a POI in A_p^l. Next, we show how to induce a_i^l in detail.

One possible way to learn a_i^l is to augment the implicit features in all its child POIs. However, different child POIs might provide different contributions when influencing the parent POIs. For example, many users may visit a shopping mall (a parent POI) frequently for a popular grocery store (a child POI) and nothing else.

To mitigate this issue, we propagate learned implicit features from a child POI h_j^{l+1} using various attention weights throughout $\mathcal{T}$ in order to learn the best inter-level feature representation a_i^l for a parent POI p_i^l. Specifically, we use a multi-layer perceptron (MLP) when learning attention weights each child POI p_j^{l+1} rooted at p_i^l.

$$\begin{cases} w_j^{l+1} = F(h_j^{l+1}) = ReLU(d(W^{l+1}h_j^{l+1} + b_1)) + b_2 \\ \tilde{w}_j^{l+1} = \sigma(w_j^{l+1}) = \dfrac{exp(w_j^{l+1})}{\sum_{p_t^{l+1} \in C(p_i^l)} exp(w_t^{l+1})} \\ a_i^l = \sum_{p_j^{l+1} \in C(p_i^l)} \tilde{w}_j^{l+1} h_j^{l+1} \end{cases} \qquad (12)$$

where the *implicit feature* embedding $h_j^{l+1} \in \mathbb{R}^{r_{l+1}}$ of child POI p_j^{l+1} is the input, and $ReLU(x) = max(0, x)$ is applied as the activation function to produce w_j^{l+1} in the first formula. $W^{l+1} \in \mathbb{R}^{d_1 \times r_{l+1}}$ is a transpose matrix, $b_1 \in \mathbb{R}^{d_1}$ denotes a bias vector, b_2 refers to a bias variable, and $d \in \mathbb{R}^{1 \times d_1}$ projects the attention weight for a POI node where the hidden layer size of the attention network is d_1. $C(p_i^l)$ indicates all child POIs rooted at p_i^l.

After computing the attention weight w_j^{l+1}, we normalize it to obtain $\tilde{w}_j^{l+1}$ using a softmax function $\sigma(\cdot)$ as shown in the second formula. Finally, a_i^l is produced using the resulting child POIs and attention weights in the third formula. The complete architecture of our attention network mechanism is depicted in the centre of Figure 2.

4.2.2 Constructing historical check-in matrix. Intuitively, a POI candidate may be recommended if it is located near a previously visited POI. To exploit spatial containment, we first construct L POI context graphs, one for each POI level. Each POI context graph embeds the contextual information of the POIs. The mechanism used to

incorporate contextual information between a POI candidate and a visited POI into our recommendation model is described next.

POI context graph. For ease of illustration, we use a single POI context graph as an example and omit superscripts (i.e., l) when denoting a particular level in $\mathcal{T}$. Specifically, we represent a POI context graph as $\mathcal{G} = \langle \mathcal{V}, \mathcal{E} \rangle$, where $\mathcal{V}$ is the set of POIs, and $\mathcal{E}$ is the set of edges between any two connected POIs. Given any two POIs p_1 and p_2 ($p_1, p_2 \in \mathcal{V}$), we define three types of edge relations, such that $\mathcal{E}$ can be further weighted using multiple geospatial influence factors.

- *Co-search.* If a user searches for a restaurant and a coffee shop within a short time interval using a map application, and then visits the restaurant, we can infer that a coffee shop has a higher likelihood of relevance the next time the user views the map [42]. Thus, we use $\delta(p_1, p_2 | \Delta t_1)$ to denote the co-occurrence search frequency between two POIs p_1 and p_2 within a fixed session interval Δt_1 (e.g., 30 minutes) for all users.
- *Co-visit.* If a user first visits a restaurant and then goes to a coffee shop and locations are being tracked for the user, we assume that the coffee shop has a higher priority for recommendations made when a user is located in a restaurant. We use $\psi(p_1, p_2 | \Delta t_2)$ to represent the visit frequency chronologically between p_1 and p_2 within a fixed time interval Δt_2 (e.g., 30 minutes).
- *Geospatial distance.* According to Tobler's first law of geography [23], "everything is related to everything else, but near things are more related than distant things". The nearby objects often have underlying relationships and influence, thus we also apply a *geospatial distance* factor which captures the geographical influence. Here, we use $\zeta(p_1, p_2)$ to denote the inverse Euclidean distance between p_1 and p_2.

Note that $\mathcal{G}$ is constructed before training. The edge weights derived using these three geospatial factors are normalized using sigmoid function, which is defined as $\sigma(x) = 1/(1 + exp(-x))$.

Graph-based geospatial influence representation. Given a POI candidate p_i to be recommended and a historical POI check-in trajectory Q^{u_k} for a user u_k, we define the geospatial influence matrix $U^l_{g,u_k} \in \mathbb{R}^{n_l \times r}$, and incorporate POI context info using Eq. 13. Since using every visited POI from Q^{u_k} is not scalable, we only choose a subset $Q^{u_k}_s$ containing the top-t frequently visited POIs from Q^{u_k} for each user u_k such that $Q^{u_k}_s \subset Q^{u_k}$ and $|Q^{u_k}_s| = t$. Specifically, we denote the embedding vector for p_i in U^l_{g,u_k} as μ^{l,p_i}_{g,u_k}, and the embedding vector for p_j in U^l_p as $v^l_{p_j}$. Thus for the recommended POI p_i and the historical visited POI p_j, we can get:

$$\mu^{l,p_i}_{g,u_k} = \frac{1}{t} \sum_{p_j \in Q^{u_k}_s} \delta(p_i, p_j | \Delta t_1) \psi(p_i, p_j | \Delta t_2) \zeta(p_i, p_j) v^l_{p_j} \quad (13)$$

where t is set to 3 in our experiment. Consequently, the embedding vector $g^l_{u_k}$ for the user u_k in the historical check-in matrix $\mathbf{G}^l$ can be computed as:

$$g^l_{u_k} = \omega_k (U^l_{g,u_k})^T \quad (14)$$

where ω_k is an embedding vector for u_k in U_u. Finally, $\mathbf{G}^l$ can be built as $\mathbf{G}^l = [\ldots, (g^l_{u_k})^T \ldots]^T$ for all users.
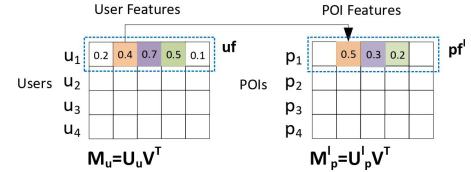
Note that POI recommendation task can be formalized as a top-k ranking problem. Once we have learned the model parameters in MPR, given a user, a ranking score for each POI located at the l-th

level of $\mathcal{T}$ can be obtained from the matrix $\mathbf{O}^l$, and then the POIs with top-k highest ranking scores will be recommended to the user.

5 HINTS FOR RECOMMENDATION JUSTIFICATION

It is desirable to complement recommendations with an intuition as to why certain results are produced, since it may not always be obvious to the user [36]. Our approach provides such additional benefit by enabling (i) *user-aspect* hint: user attributes used by the model can be derived; (ii) *POI-aspect* hint: when a parent POI is recommended, specific child POIs can be discovered; and (iii) *interaction-aspect* hint: if we recommend a new POI, we can highlight data from historical check-in venues that were most relevant.

User-aspect. We assume that a user u_i has visited a POI p_j based on the attributes of that POI. Our model captures the top-K features for u_i from an explicit feature embedding vector $\mathbf{uf}$, obtained from a row vector from $\mathbf{M}_u$ matrix, which is computed by $\mathbf{M}_u = \mathbf{U}_u \mathbf{V}^T$ (as mentioned in Section 3). K is set to 5 in our experiment. Thus, the column index set $B_i = \langle b_{i1}, b_{i1}, ..., b_{iK} \rangle$ are the top-K ranked in $\mathbf{uf}$. The matrix $\mathbf{M}^l_p = \mathbf{U}^l_p \mathbf{V}^T$ is used to determine the POI explicit feature embedding vector $\mathbf{pf}^l$ and find the corresponding POI feature prediction values based on B_i. We can then expose the POI feature with the highest value to u_i for recommendation evidence.

Figure 3: Illustration example on user-aspect hint.

An illustrative example of a user-aspect hint is shown in Figure 3. After obtaining the two matrices $\mathbf{M}_u$ and $\mathbf{M}^l_p$, say for the user u_1, the user feature with the highest K values (assuming that $K = 3$, then $B_1 = \langle 2, 3, 4 \rangle$) is located in the second, third, and fourth column using the embedding $\mathbf{uf}$. Then, the corresponding POI features whose column indexes drop into B_1 are identified, where the POI feature with the highest value 0.5 in the second column of $\mathbf{pf}^l$ can then be presented as a hint to the user.

POI-aspect. Intuitions about parent POI recommendations can be derived from the attention influence weights computed for each child POI (as described in Section 4.2.1). If we recommend a parent POI p to a user u_i, a set of important child POIs can be shown, ordered by attention scores. Thus the contribution ratio for each child POI p_j ($p_j \in C(p)$) over all child POIs $C(p)$ is computed by $\frac{\mathbf{a_{u_i}} \odot \mathbf{a_{p_j}}}{\sum_{p_c \in C(p_j)} \mathbf{a_{u_i}} \odot \mathbf{a_{p_c}}}$, where $\mathbf{a_{u_i}}$ is a user embedding in $\mathbf{A}^l_u$, $\mathbf{a_{p_j}}$ and $\mathbf{a_{p_c}}$ are two POI embedding vectors in $\mathbf{A}^l_p$, and $\odot$ is the dot product operator. We mark the child POI with the highest contribution ratio as a "hot" POI which might attract the user.

Interaction-aspect. For any recommended POI p_j, we can easily evaluate the contribution to examine whether the historical check-in information influences the final prediction. We define the contribution ratio as the prediction score $\mathbf{G}^l_{u_i, p_j}$ (as introduced in Section 4.2.2) on historical interactions divided by the total predicted score $\mathbf{O}^l_{u_i, p_j}$, which is $\gamma = \frac{\mathbf{G}^l_{u_i, p_j}}{\mathbf{O}^l_{u_i, p_j}}$. If γ exceeds a threshold,

we assume that the historical check-in information is the important contributor when recommending p_j to u_i.

6 EXPERIMENTAL STUDY

We investigate the following four research questions:

- **RQ1.** How does our proposed MPR model perform when compared with the state-of-the-art POI recommendation methods?
- **RQ2.** How does MPR perform when varying the hyper-parameter settings (e.g., *embedding size*)?
- **RQ3.** How can MPR be used to provide recommendation hints?
- **RQ4.** How do different components in MPR contribute to the overall performance?

We evaluate all methods using two real-world city-wide datasets, *Beijing* and *Chengdu*, from Baidu Maps[1], which is one of the most popularly used map services in China. Both datasets are randomly sampled as a portion of whole data from Baidu Maps. Due to space limitations, we only show the experimental results for the *Beijing* dataset, except when answering **RQ1**. Similar performance trends were observed for the *Chengdu* dataset when answering RQ2-RQ4.

- *The POI tree $\mathcal{T}$.* We trace the profile for each POI and then recursively search its parent POI to build $\mathcal{T}$. A three-level POI tree is built: H_1, H_2, and H_3 from top to bottom. For example, a spatial containment path in $\mathcal{T}$ on the *Beijing* dataset is *Wudaokou* (a famous neighborhood in *Beijing*)→*Tsinghua University*→*Tsinghua Garden*, which are located at H_1, H_2, and H_3, respectively.
- *Check-in data.* Each check-in has the following info: userId, poiId and a check-in timestamp. We filter out users with fewer than 10 check-in POIs and POIs visited by fewer than 10 users. To build the check-in data on H_1 and H_2, the check-in records from users was used and we also aggregated the check-ins in the parent POIs if any of their child POIs were visited.
- *User and POI profile.* Each user has their own attributes such as age and hobby, and f_u =173 user features are extracted. Each POI has a parent POI, and its own attributes, where f_p =467 representative POI features are available after filtering out those attributes shared by fewer than 10 POIs.

Setup. We partitioned the check-in data into a training set, a validation set, and a test set. The first two months of check-ins were used for training in the *Beijing* testset, and the first three months in *Chengdu*. The most recent 15 days of check-ins were used as the test data and all remaining ones were used in the validation data in both datasets. A negative sample was randomly selected for each positive sample during training. Any check-in that occurred in the training set was pruned from both the validation and test set, to ensure that any POI recommended had never been visited by the user before.

For each model, the parameters were tuned on the validation data to find the best values that maximized $P@k$, and used for all test predictions. Mini-batch adaptive gradient descent [6] is used to control the learning step size dynamically. All experiments were implemented in Python on a GPU-CPU platform using a GTX 1080 GPU.

Evaluation Metrics. We adopt two commonly-used performance metrics [18]: Precision ($P@k$), and Normalized Discounted Cumulative Gain ($NDCG@k$). These two metrics were used to evaluate the model performance since $P@k$ is commonly used when evaluating the coverage of recommendation results, and $NDCG@k$ captures additional signals about the overall effectiveness of the top-k recommendations, and supports graded relevance.

Parameter Settings. The parameters Δt_1 and Δt_2 are set to 30 minutes by default. The adjustable parameter τ for graph-based geospatial influence is set to 1 by default, and the regularization parameters are set as follows: $\lambda_1 = 0.01$ and $\lambda_2 = 0.1$, both of which are set according to the experiment evaluation using the validation dataset. Furthermore, the hidden factor size r_l of the POI levels are fixed, and we empirically set the attention layer size d_1 to be the same as r_l, which is equal to 150 discovered during the parameter tuning experiment shown in Table 3.

6.1 Overview

Baselines. To validate the performance of our model MPR, we compared directly against the following state-of-the-art methods. Note that, these baselines all treat POIs as isomorphic, thus we have to construct multiple models, one for each POI level, in order to generate comparable output to our approach.

- WRMF (Weighted Regularized Matrix Factorization) [10]: a pointwise latent factor model that distinguishes user observed and unobserved check-in data by using confidence values to adapt to implicit feedback data from a user.
- BPRMF (Bayesian Personalized Ranking) [22]: a pair-wise learning framework for implicit feedback data, combined with matrix factorization as the internal predictor.
- PACE (Preference and Context Embedding) [29]: a neural embedding approach that generally combines user check-in behaviors and context information from users and POIs through a graph-based semi-supervised learning framework.
- SAE-NAD (Self-attentive Autoencoders with Neighbor-Aware Influence) [20]: explicitly integrates spatial information into an autoencoder framework and uses a self-attention mechanism to generate user representation from historical check-in records.

6.2 Effectiveness Comparisons (RQ1)

6.2.1 Baseline Comparisons. Table 2 compares all methods using different k values on both datasets. The key observations can be summarized as follows.

- Our model MPR achieves the best performance on all metrics at every single level of spatial granularity, demonstrating the robustness of our model. Specifically, the NDCG@10 for MPR on *Beijing* has: (1) a 4.5% improvement over the best baseline SAE-NAD at the H_1 level; (2) a 4.5% improvement over the strongest baseline WRMF at the H_2 level; and (3) a 5% improvement over the best baseline SAE-NAD at the H_3 level.
- In term of P@10, MPR substantially outperforms WRMF and BPRMF (42.6% and 4.7% respectively) at the H_1 level. This results from WRMF and BPRMF treating each POI level independently when training the model. Clearly, MPR benefits from jointly optimizing the loss for every level of $\mathcal{T}$ in order to achieve its collaborative training goal.

Table 2: Model performance comparisons on the *Beijing* and *Chengdu* dataset. Entries marked $^\triangle$ and $^\blacktriangle$ correspond to statistical significance using a paired t-test with Bonferroni correction at 95% and 99.9% confidence intervals respectively. Comparisons are relative to PACE.

Level	Model	Beijing						Chengdu					
		P@5	NDCG@5	P@10	NDCG@10	P@20	NDCG@20	P@5	NDCG@5	P@10	NDCG@10	P@20	NDCG@20
H_1	WRMF	0.056▼	0.096▼	0.047▼	0.121▼	0.037▼	0.151▼	0.063▼	0.079▼	0.051▼	0.098▼	0.041▼	0.127▼
	BPRMF	0.079▲	0.123▲	0.064▲	0.150▲	0.050▲	0.187▲	0.110▲	0.142▲	0.086▲	0.170▲	0.061▲	0.202▲
	PACE	0.067	0.104	0.053	0.124	0.043	0.156	0.087	0.117	0.074	0.152	0.054	0.181
	SAE-NAD	0.078▲	0.125▲	0.064▲	0.155▲	0.051▲	0.194▲	0.100▲	0.128▲	0.081▲	0.155▲	0.057▲	0.185▲
	MPR	**0.084**▲	**0.133**▲	**0.067**▲	**0.162**▲	**0.053**▲	**0.203**▲	**0.119**△	**0.159**△	**0.094**▲	**0.190**▲	**0.064**▲	**0.222**▲
H_2	WRMF	0.009	0.017	0.007	0.022	0.005	0.026▲	0.022	0.027	0.018▽	0.034	0.013	0.040
	BPRMF	0.007	0.014▲	0.007	0.020▲	0.005	0.026▲	0.027	0.037	0.022	0.047	0.017	0.058
	PACE	0.007	0.013	0.007	0.019	0.005	0.024	0.022	0.031	0.022	0.039	0.013	0.046
	SAE-NAD	0.007	0.014▲	0.006▼	0.018▼	0.005	0.024	**0.033**	0.043	0.019	0.049	0.017	0.059
	MPR	**0.010**▲	**0.018**▲	**0.008**▲	**0.023**▲	**0.007**▲	**0.030**▲	**0.033**▲	**0.044**▲	**0.026**△	**0.054**▲	**0.020**▲	**0.067**▲
H_3	WRMF	0.008▲	0.015▲	0.006▲	0.018▲	0.004	0.022▲	0.021△	0.027△	0.017	0.033	0.013	0.041
	BPRMF	0.006▼	0.012▲	0.005	0.015▲	0.004	0.019▲	0.021△	0.029	0.017	0.036	0.013△	0.043▲
	PACE	0.007	0.008	0.005	0.009	0.004	0.010	0.016	0.023	0.016	0.032	0.009	0.035
	SAE-NAD	0.008▲	0.015▲	0.007▲	0.020▲	0.005▲	**0.026**▲	0.020▲	0.027▲	0.020△	0.038▲	0.016▲	0.047▲
	MPR	**0.009**▲	**0.015**▲	**0.007**▲	**0.021**▲	**0.006**▲	**0.026**▲	**0.032**▲	**0.042**▲	**0.021**▲	**0.046**▲	**0.016**▲	**0.056**▲

Table 3: Impact of Parameters τ and r_l on *Beijing* dataset

Level	Metric	τ			r_l		
		0.6	1	1.4	50	150	250
H_1	P@10	0.067	0.067	**0.068**	0.065	0.067	**0.068**
	NDCG@10	0.161	**0.162**	0.162	0.153	**0.162**	0.162
H_2	P@10	0.007	**0.008**	0.008	0.008	**0.008**	0.008
	NDCG@10	0.021	**0.023**	0.023	0.021	**0.023**	0.023
H_3	P@10	0.007	**0.007**	0.007	0.006	**0.007**	0.007
	NDCG@10	0.018	**0.021**	0.019	0.018	**0.021**	0.020

Table 4: Ablation study on the *Beijing* dataset.

Level	Metric	M1	M2	M3
H_1	P@10	0.066	0.067	0.067
	NDCG@10	0.156	0.160	0.162
H_2	P@10	0.007	0.008	0.008
	NDCG@10	0.020	0.022	0.023
H_3	P@10	0.006	0.006	0.007
	NDCG@10	0.010	0.011	0.021

- Both PACE and SAE-NAD directly incorporate geospatial distance information. We can observe that SAE-NAD outperforms PACE in most cases. One potential reason is that although PACE builds a context graph to model important geographical influences, it ignores the historical visit information when extracting the POI-POI co-visit relations that are used by SAE-NAD. However, SAE-NAD employs an autoencoder and self-attention mechanism when constructing POI-and-POI relations, while our model MPR is able to learn the geospatial influence relations across all $\mathcal{T}$ levels, and the additive benefits are clear. As such, we believe that the inter-level relations captured by our model are both flexible and effective.

- We performed a Bonferroni corrected paired t-test and show the significance across all three levels for all four baselines. Comparisons were relative to PACE, which has recently been adapted to solve several different location-based recommendation problems.

6.2.2 Tree Level Effects in MPR. We also found that MPR performs relatively well at both H_1 and H_2 levels, since the upper level captures much richer information from the lower levels using the attention mechanism. Implicit feature representations of child POIs are aggregated from child to parent, increasing the data available when learning the new model. In contrast, for POIs at the H_3 level, these signals are not available, and thus the overall performance compared with the other baselines exhibits less dramatic performance improvements, but is still effective.

6.3 Hyper-parameter Studies (RQ2)

6.3.1 Impact of Matrix Tradeoff Parameter. Table 3 shows the results when varying τ (in Eq. 10) from 0.6 to 1.4, in order to control the tradeoff between the feature-based check-in matrix and history-based check-in matrix. With the increase of τ, the effectiveness $NDCG@10$ of POI recommendations at H_2 and H_3 are more sensitive than that at H_1. From the results, we observe that the $NDCG@10$ at the H_3 level first goes up, and then begins to drop off. Considering the holistic performance for all these three levels, our model adopts the setting $\tau = 1$ that achieves its best overall performance.
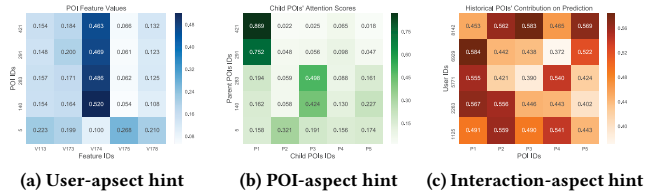
6.3.2 Impact of Embedding Size. We also investigated the performance when varying the embedding size r_l from 50 to 250 in Table 3. The $NDCG@10$ of both H_1 and H_2 improved as expected since these levels have access to additional information from the lower levels. However, although the precision of H_1 and H_2 peak when $r_l = 250$, the model training costs are higher and may be more prone to overfitting. In the remaining experiments, we chose $r_l = 150$ since it offered the best trade-off based on our internal experiments.

6.4 Recommendation Hints (RQ3)

We analyzed our model and created several heat maps to demonstrate how recommendation hints might be created in Figure 4. All values are min-max normalized for direct comparisons in the figure.

6.4.1 User-aspect hint. Figure 4a illustrates the POI feature prediction values, where a row represents a recommended POI, and a

| (a) User-aspect hint | (b) POI-aspect hint | (c) Interaction-aspect hint |

Figure 4: Visualization heat maps of three recommendation hints on the *Beijing* dataset. The larger a value is, the darker color its corresponding cell has.

column denotes a POI feature. In the figure, users were randomly sampled and we selected five user features which best represented the sampled user preferences according to the learned user feature prediction matrix $\mathbf{M}_u$. Then we recorded the column numbers, which are V113, V173, V174, V175, and V178. We then recommended five POIs (i.e., 5, 140, 283, 291, and 421), and extracted the POI feature prediction values from the learned POI feature prediction matrix $\mathbf{M}_p^l$ by the corresponding recorded columns accordingly (e.g., V113). When examining the heatmap of the resulting POI feature values, we can clearly observe the POI feature which has the highest value. For example, when we recommended POI 421st to the user, the V174 feature had the greatest contribution.

6.4.2 POI-aspect hint. Figure 4b depicts the child POI attention scores, where a row represents a recommended parent POI, and a column denotes a child POI. Specifically, we first chose the top-5 parent POIs recommended to a user. For each recommended parent POI, we analyzed the attention scores and displayed the top-5 child POIs ($P1$-$P5$) that had the highest attention score. The score contribution ratios for each child POI are then displayed. The child POI with the highest attention score can be interpreted as follows. When POI 421*st* was recommended, we can observe that it had a child POI $P1$ that was also important for that user.

6.4.3 Interaction-aspect hint. Figure 4c shows the contribution percentages (i.e., γ) from the historical POIs used in the overall prediction, where a row refers to a user, and a column is a recommended POI. In this experiment, we randomly chose five users. For each user, we produce five recommended POIs ($P1$-$P5$). If γ w.r.t. a historical POI exceeds a fixed threshold (say 0.5), then we consider this historical POI to be a strong influence on the final prediction. Using the 1125*th* user as a concrete example, the geospatial influence from historical POIs had a strong influence on the recommendations of $P2$ and $P4$.

6.5 Ablation Study (RQ4)

In this section, we present an ablation study to better understand the influence of two core submodules: (i) child POI features propagated to a parent POI bottom-up using the attention mechanism (Section 4.2.1); (ii) the geospatial influence factors between POIs derived from a POI context graph, which map three different sources of spatial relationships between any two POIs at the same POI level (Section 4.2.2). We evaluated three variants of models with or without the above core submodules: (1) M1: our model without both submodules (i) and (ii); (2) M2: our model without submodule (ii); (3) M3: our model MPR. The experimental results when $k = 10$ are shown in Table 4. When comparing the model M1 with M2, we find that the attention network mechanism indeed provides a

substantial effectiveness improvement in most cases. Although H_3 lacks the propagated child POI features, the joint training across all POI levels still provides additional performance benefits. When comparing M2 and M3, we find that M3 also achieves consistent performance improvements for $NDCG@10$, reaffirming the importance of geospatial influence in the POI context graph.

7 RELATED WORK

POI recommendation has been intensively studied in recent years, with a focus on how to integrate spatial and temporal properties [30, 33, 34]. Recent advances in machine learning techniques have inspired several innovative methods, such as sequential embedding [39], graph-based embedding [28], autoencoder-based models [20] and semi-supervised learning methods [29]. We refer the interested readers to a comprehensive survey [18] on POI recommendation. In the remainder of this section, we review the most closely related work to our own.

Category-aware POI Recommendation. Categories of POIs visited by a user often capture preferred activities, thus they are important indicators to model user preferences [16, 27, 41]. Liu et al. [17] exploited the transition patterns of user preferences over location categories to enhance recommendation performance. Specifically, a POI category tree is built, where the top level has *food* or *entertainment*, while the bottom level includes *Asian restaurant* or *bar*. Zhao et al. [38] showed that a POI has different influences in different sub-categories. Based on the hierarchical categories of each POI, they devised a geographical matrix factorization method (which is a variant of GeoMF [14]) for recommendation. The essential difference is that, each POI in [38] is still a single node but with multiple influence areas for hierarchical categories, whereas in our problem a POI has a tree structure constructed by spatial containment relationship. He et al. [9] adopted a two-step mode in their model, which predicted the category preference of next POI first and then derived the ranking list of POIs within the corresponding category.

However, these studies differ from our work. They maintain a hierarchical structure of POI categories, but we focus on how to exploit the spatial containment, rather than semantic categories.

Recommendation based on a Spatial Hierarchy. The utility of exploiting hierarchical structures of either users or items for item recommendation has been discussed in several prior studies [19, 25, 35]. Here we mainly highlight the key difference between existing approaches involving spatial hierarchy and ours.

Yin et al. [32] split the whole geographical area into a spatial pyramid of varying grid cells at different levels. The main purpose of such a spatial pyramid was to overcome the data sparsity problem. If the check-in data w.r.t. a region is sparse, then the check-in data generated by its ancestor regions can be used. Feng et al. [7] proposed a latent representation model to incorporate geographical influence, where all POIs are divided into different regions hierarchically and a binary tree is built over the POIs in each region. One major difference is that they aim to predict a set of users who will visit a given POI in a given future period. Chang et al. [4] proposed a hierarchical POI embedding model from two data layers (i.e., a check-in context layer and a text content layer), neither of which is related with the tree structure of POIs in our work. Zheng et al. [40] leveraged the hierarchy property of geographic spaces to mine user similarity by exploring people's movements on different scales of

geographic spaces. They assume that users who share similar location histories on geographical spaces of finer granularities may be more correlated. Therefore, these methods are not straightforward to cope with our multi-level POI recommendation problem.

In summary, we are the first to define the multi-level POI recommendation problem, and utilize a POI hierarchical tree structure based on spatial containment to achieve POI recommendations from varying spatial granularity.

8 CONCLUSION

In this work, we proposed and studied the multi-level POI recommendation problem. We show how to create POI recommendations at varying levels of spatial granularity by constructing a POI tree, derived from various spatial containment relationships between items. Different from existing POI recommendation studies which support the next-POI recommendation, we provide more recommendation strategies which can be used directly by a wide variety of geographically based recommendation engines. To address this problem, we proposed a multi-task learning model called MPR, where each task seamlessly combines two subtasks: attribute-based representation learning and interaction-based representation learning. We also provide three different recommendation hint types which can be produced using our model. Finally, we compared our model with several state-of-the-art approaches and two real-world datasets, thus demonstrating the effectiveness of our new approach. In future work, we will explore techniques to incorporate temporal information into our model and further boost the effectiveness.

REFERENCES

[1] Jie Bao, Yu Zheng, David Wilkie, and Mohamed Mokbel. 2015. Recommendations in location-based social networks: a survey. *GeoInformatica* 19, 3 (2015), 525–565.
[2] Ramesh Baral and Tao Li. 2017. PERS: A Personalized and Explainable POI Recommender System. *arXiv preprint arXiv:1712.07727* (2017).
[3] Ramesh Baral, XiaoLong Zhu, SS Iyengar, and Tao Li. 2018. ReEL: Review Aware Explanation of Location Recommendation. In *UMAP*. 23–32.
[4] Buru Chang, Yonggyu Park, Donghyeon Park, Seongsoon Kim, and Jaewoo Kang. 2018. Content-Aware Hierarchical Point-of-Interest Embedding Model for Successive POI Recommendation.. In *IJCAI*. 3301–3307.
[5] Mostafa Dehghani, Hamed Zamani, Aliaksei Severyn, Jaap Kamps, and W Bruce Croft. 2017. Neural ranking models with weak supervision. In *SIGIR*. 65–74.
[6] John Duchi, Elad Hazan, and Yoram Singer. 2011. Adaptive subgradient methods for online learning and stochastic optimization. *JMLR* 12 (2011), 2121–2159.
[7] Shanshan Feng, Gao Cong, Bo An, and Yeow Meng Chee. 2017. Poi2vec: Geographical latent representation for predicting future visitors. In *AAAI*. 102–108.
[8] Mengyue Hang, Ian Pytlarz, and Jennifer Neville. 2018. Exploring student check-in behavior for improved point-of-interest prediction. In *SIGKDD*. 321–330.
[9] Jing He, Xin Li, and Lejian Liao. 2017. Category-aware Next Point-of-Interest Recommendation via Listwise Bayesian Personalized Ranking. In *IJCAI*. 1837–1843.
[10] Yifan Hu, Yehuda Koren, and Chris Volinsky. 2008. Collaborative filtering for implicit feedback datasets. In *ICDM*. 263–272.
[11] Yehuda E Kalay. 1982. Determining the spatial containment of a point in general polyhedra. *Computer Graphics and Image Processing* 19, 4 (1982), 303–334.
[12] Huayu Li, Yong Ge, Richang Hong, and Hengshu Zhu. 2016. Point-of-interest recommendations: Learning potential check-ins from friends. In *SIGKDD*. 975–984.
[13] Xutao Li, Gao Cong, Xiao-Li Li, Tuan-Anh Nguyen Pham, and Shonali Krishnaswamy. 2015. Rank-geofm: A ranking based geographical factorization method for point of interest recommendation. In *SIGIR*. 433–442.
[14] Defu Lian, Cong Zhao, Xing Xie, Guangzhong Sun, Enhong Chen, and Yong Rui. 2014. GeoMF: joint geographical modeling and matrix factorization for point-of-interest recommendation. In *SIGKDD*. 831–840.
[15] Bin Liu, Hui Xiong, Spiros Papadimitriou, Yanjie Fu, and Zijun Yao. 2014. A general geographical probabilistic factor model for point of interest recommendation. *TKDE* 27, 5 (2014), 1167–1179.
[16] Hao Liu, Yongxin Tong, Panpan Zhang, Xinjiang Lu, Jianguo Duan, and Hui Xiong. 2019. Hydra: A Personalized and Context-Aware Multi-Modal Transportation Recommendation System. In *SIGKDD*. 2314–2324.
[17] Xin Liu, Yong Liu, Karl Aberer, and Chunyan Miao. 2013. Personalized point-of-interest recommendation by mining users' preference transition. In *CIKM*. 733–738.
[18] Yiding Liu, Tuan-Anh Nguyen Pham, Gao Cong, and Quan Yuan. 2017. An experimental evaluation of point-of-interest recommendation in location-based social networks. *PVLDB* 10, 10 (2017), 1010–1021.
[19] Kai Lu, Guanyuan Zhang, Rui Li, Shuai Zhang, and Bin Wang. 2012. Exploiting and exploring hierarchical structure in music recommendation. In *AIRS*. 211–225.
[20] Chen Ma, Yingxue Zhang, Qinglong Wang, and Xue Liu. 2018. Point-of-Interest Recommendation: Exploiting Self-Attentive Autoencoders with Neighbor-Aware Influence. In *CIKM*. 697–706.
[21] Tuan-Anh Nguyen Pham, Xutao Li, and Gao Cong. 2017. A general model for out-of-town region recommendation. In *WWW*. 401–410.
[22] Steffen Rendle, Christoph Freudenthaler, Zeno Gantner, and Lars Schmidt-Thieme. 2009. BPR: Bayesian personalized ranking from implicit feedback. In *UAI*. 452–461.
[23] Waldo R Tobler. 1970. A computer movie simulating urban growth in the Detroit region. *Economic geography* 46 (1970), 234–240.
[24] Hao Wang, Huawei Shen, Wentao Ouyang, and Xueqi Cheng. 2018. Exploiting POI-Specific Geographical Influence for Point-of-Interest Recommendation. In *IJCAI*. 3877–3883.
[25] Suhang Wang, Jiliang Tang, Yilin Wang, and Huan Liu. 2015. Exploring Implicit Hierarchical Structures for Recommender Systems.. In *IJCAI*. 1813–1819.
[26] Weiqing Wang, Hongzhi Yin, Zi Huang, Qinyong Wang, Xingzhong Du, and Quoc Viet Hung Nguyen. 2018. Streaming ranking based recommender systems. In *SIGIR*. 525–534.
[27] Yuan Xia, Jingbo Zhou, Jingjia Cao, Yanyan Li, Fei Gao, Kun Liu, Haishan Wu, and Hui Xiong. 2018. Intent-aware audience targeting for ride-hailing service. In *ECML/PKDD*. 136–151.
[28] Min Xie, Hongzhi Yin, Hao Wang, Fanjiang Xu, Weitong Chen, and Sen Wang. 2016. Learning graph-based poi embedding for location-based recommendation. In *CIKM*. 15–24.
[29] Carl Yang, Lanxiao Bai, Chao Zhang, Quan Yuan, and Jiawei Han. 2017. Bridging collaborative filtering and semi-supervised learning: a neural approach for poi recommendation. In *SIGKDD*. 1245–1254.
[30] Zijun Yao, Yanjie Fu, Bin Liu, Yanchi Liu, and Hui Xiong. 2016. POI recommendation: A temporal matching between POI popularity and user regularity. In *ICDM*. 549–558.
[31] Mao Ye, Peifeng Yin, Wang-Chien Lee, and Dik-Lun Lee. 2011. Exploiting geographical influence for collaborative point-of-interest recommendation. In *SIGIR*. 325–334.
[32] Hongzhi Yin, Weiqing Wang, Hao Wang, Ling Chen, and Xiaofang Zhou. 2017. Spatial-aware hierarchical collaborative deep learning for POI recommendation. *TKDE* 29, 11 (2017), 2537–2551.
[33] Quan Yuan, Gao Cong, Zongyang Ma, Aixin Sun, and Nadia Magnenat Thalmann. 2013. Time-aware point-of-interest recommendation. In *SIGIR*. 363–372.
[34] Quan Yuan, Gao Cong, and Aixin Sun. 2014. Graph-based point-of-interest recommendation with geographical and temporal influences. In *CIKM*. 659–668.
[35] Weijia Zhang, Hao Liu, Yanchi Liu, Jingbo Zhou, and Hui Xiong. 2020. Semi-Supervised Hierarchical Recurrent Graph Neural Network for City-Wide Parking Availability Prediction. In *AAAI*.
[36] Yongfeng Zhang and Xu Chen. 2018. Explainable Recommendation: A Survey and New Perspectives. *arXiv preprint arXiv:1804.11192* (2018).
[37] Yongfeng Zhang, Guokun Lai, Min Zhang, Yi Zhang, Yiqun Liu, and Shaoping Ma. 2014. Explicit factor models for explainable recommendation based on phrase-level sentiment analysis. In *SIGIR*. 83–92.
[38] Pengpeng Zhao, Xiefeng Xu, Yanchi Liu, Ziting Zhou, Kai Zheng, Victor S Sheng, and Hui Xiong. 2017. Exploiting Hierarchical Structures for POI Recommendation. In *ICDM*. 655–664.
[39] Shenglin Zhao, Tong Zhao, Irwin King, and Michael R Lyu. 2017. Geo-teaser: Geo-temporal sequential embedding rank for point-of-interest recommendation. In *WWW*. 153–162.
[40] Yu Zheng, Lizhu Zhang, Zhengxin Ma, Xing Xie, and Wei-Ying Ma. 2011. Recommending friends and locations based on individual location history. *TWEB* 5, 1 (2011), 5:1–5:44.
[41] Jingbo Zhou, Shan Gou, Renjun Hu, Dongxiang Zhang, Jin Xu, Airong Jiang, Ying Li, and Hui Xiong. 2019. A Collaborative Learning Framework to Tag Refinement for Points of Interest. In *SIGKDD*. 1752–1761.
[42] Jingbo Zhou, Hongbin Pei, and Haishan Wu. 2018. Early warning of human crowds based on query data from Baidu maps: Analysis based on Shanghai stampede. In *Big data support of urban planning and management*. 19–41.